

# Micellar Formation of Poly( $\epsilon$ -caprolactone-*block*-ethylene oxide-*block*-caprolactone) and Its Enzymatic Biodegradation in Aqueous Dispersion

Ting Nie,<sup>†</sup> Yue Zhao,<sup>‡</sup> Zuwei Xie,<sup>\*,†,§</sup> and Chi Wu<sup>\*,†,§</sup>

Shanghai-Hong Kong Joint Laboratory in Chemical Synthesis, Shanghai Institute of Organic Chemistry, Chinese Academy of Sciences, 354 Fenglin Lu, Shanghai 200032, China;

The Open Laboratory of Bond-Selective Chemistry, Department of Chemical Physics, University of Science and Technology of China, Hefei, Anhui, China; and

Department of Chemistry, The Chinese University of Hong Kong, Shatin, N.T., Hong Kong

Received August 4, 2003; Revised Manuscript Received September 16, 2003

**ABSTRACT:** The water-insoluble triblock copolymer poly( $\epsilon$ -caprolactone-*b*-ethylene oxide-*b*- $\epsilon$ -caprolactone) (PCL-*b*-PEO-*b*-PCL) can form core-shell-like polymeric micelles in aqueous solution where the core and shell are respectively made of collapsed hydrophobic PCL and swollen hydrophilic PEO blocks. Four PCL-*b*-PEO-*b*-PCL triblock copolymers with different PEO/PCL molar ratios were prepared and characterized. The degradation of these copolymer micelles in the presence of enzyme lipase PS was much faster than the bulk PCL or PCL thin film. The degradation kinetics was investigated using a combination of laser light scattering and pH measurements. The results revealed that the in-situ biodegradation of the copolymer chains inside the micelle could be effectively monitored by a pH meter, while laser light scattering measures the biodegradation-induced dissociation of the micelles in water. The effects of the enzyme and copolymer concentrations as well as the PCL/PEO molar ratios on the biodegradation kinetics were studied.

## Introduction

Biodegradable and biocompatible polymers have been widely used in biomedical applications and colloidal science,<sup>1</sup> including poly(lactic acid) (PLA), poly(glycolic acid) (PGA), poly( $\epsilon$ -caprolactone) (PCL), and their copolymers.<sup>2</sup> One of the biomedical applications is controllable drug-delivery devices because they are completely degradable inside the body after the interaction with body fluid, enzyme, and cells.<sup>3</sup> The resultant low molar mass molecules during the biodegradation can be either absorbed by the body or removed by metabolism. For a given type of polymers, the biodegradation rate and releasing kinetics of loaded drugs can be adjusted by its chemical composition and molar mass.<sup>4</sup> Therefore, the study of the biodegradation kinetics is essentially important for applications of biodegradable polymers. More specifically, for the application of injection, drugs have to be encapsulated on wrapped inside biodegradable polymeric microspheres with a uniform size smaller than blood vessels.

The micellar formation of block or graft copolymers in a selective solvent is one way to prepare polymeric nanoparticles.<sup>5–8</sup> It has been shown that the water-insoluble triblock copolymer poly( $\epsilon$ -caprolactone-*b*-ethylene oxide-*b*- $\epsilon$ -caprolactone) (PCL-*b*-PEO-*b*-PCL) can form polymeric micelles stable in aqueous solution. The particles have a collapsed hydrophobic PCL core and a swollen hydrated PEO shell.<sup>9,10</sup> In this follow-up study, four PCL-*b*-PEO-*b*-PCL triblock copolymers with different PEO and PCL molar ratios were synthesized, characterized, and micellized. The degradation of these PCL-*b*-PEO-*b*-PCL micelles in the presence of enzyme lipase PS can be investigated by laser light scattering

(LLS).<sup>11</sup> In comparison with other traditional methods, such as weighting or oxygen consumption, the LLS method offers several advantages, such as nonintrusive, fast, and accurate. Since the degradation of these copolymers results in low molar mass acids, the values of pH decrease as the degradation proceeds. Therefore, we decided to monitor the degradation by a combination of LLS and pH measurements, which provides a better understanding of the biodegradation kinetics.

## Experimental Section

**Sample Preparation.** All chemicals, except otherwise stated, were purchased from Aldrich Chemical Co. Lipase PS from *Pseudomonas cepacia* (courtesy of Amano Pharmaceutical, Japan) was further purified by freeze-drying. <sup>1</sup>H NMR (Bruker AM-300) spectra of the copolymers were recorded in CDCl<sub>3</sub> at room temperature. The copolymer compositions were estimated from the ratio of the peak areas assigned to PEO and PCL blocks in the NMR spectrum. As the number-average molar mass of the PEO blocks is known, we can estimate the number-average molar mass of the two PCL blocks from the NMR peaks. The values of pH of the polymeric micelle dispersion were in situ recorded by a conventional pH meter equipped with a digital recording device.

Four triblock PCL-*b*-PEO-*b*-PCL copolymers with different PEO/PCL mass ratios (10%–46%) were synthesized by ring-opening polymerization of a prescribed amount of  $\epsilon$ -caprolactone (CL) initiated by poly(ethylene glycol) ( $M_w = 1.0 \times 10^4$  g/mol) at 130 °C in the presence of stannous octoate as catalyst. The reaction was carried for 27 h (Scheme 1). The synthetic details can be found elsewhere.<sup>12</sup> The copolymers were purified and are denoted hereafter as PCL46, PCL35, PCL19, and PCL10 according to their PCL mass percents. The values of the mass ratio [PEO]/[PCL], the molar number of PEO and PCL monomer units, and apparent weight-averaged molar mass  $M_w$  of these triblock copolymers are summarized in Table 1. The polydispersity index of PCL blocks is  $\sim 1.3$ .

The micellar formation involves a process of adding dropwise 1 mL of a dilute THF solution ( $1.0 \times 10^{-2}$  g/mL) of PCL-*b*-PEO-*b*-PCL copolymer into 100 mL of water under a magnetic stirring. As soon as the copolymer solution is added, THF

<sup>†</sup> Shanghai-Hong Kong Joint Laboratory in Chemical Synthesis.

<sup>‡</sup> University of Science and Technology of China.

<sup>§</sup> The Chinese University of Hong Kong.

\* Corresponding authors: e-mail zxie@cuhk.edu.hk; chiwu@cuhk.edu.hk.

**Scheme 1. Schematic of Synthesis of PCL-*b*-PEO-*b*-PCL Triblock Copolymer**

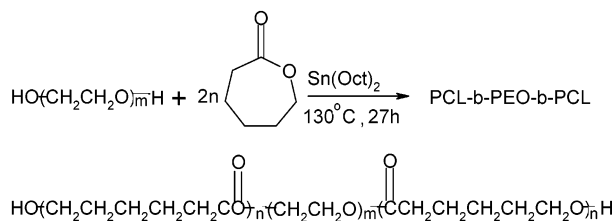


**Table 1. Laser Light Scattering Characterization of Triblock Copolymers PCL-*b*-PEO-*b*-PCL Molecular Parameters<sup>a</sup> as Well as Their Nanoparticles in Water at 37 °C**

sample	PCL46	PCL35	PCL19	PCL10
$W_{PEO}/W_{PCL}$	54/46	65/35	81/19	90/10
$n_{PEO}/n_{PCL}$	227/75	227/47	227/20	227/9
$M_w/(g/mol)$	$1.9 \times 10^4$	$1.5 \times 10^4$	$1.2 \times 10^4$	$1.1 \times 10^4$
$M_{w,PCL}/(g/mol)$	$8.6 \times 10^3$	$5.4 \times 10^3$	$2.3 \times 10^3$	$9.8 \times 10^2$
$M_{w,PEO}/(g/mol)$	$1.0 \times 10^4$	$1.0 \times 10^4$	$1.0 \times 10^4$	$1.0 \times 10^4$
$M_{w,particle}/(g/mol)$	$6.9 \times 10^7$	$1.2 \times 10^7$		
$\langle R_g \rangle/nm$	107	78		
$\langle R_h \rangle/nm$	95	74	80/10	
$\langle R_g \rangle/\langle R_h \rangle$	1.1	1.1		
$N_{aggregation}$	$3.6 \times 10^3$	$8.0 \times 10^2$		

<sup>a</sup> By <sup>1</sup>H NMR. The relative errors:  $\langle M_w \rangle$ ,  $\pm 5\%$ ;  $\langle R_g \rangle$ ,  $\pm 8\%$ ;  $\langle R_h \rangle$ ,  $\pm 2\%$ .

quickly diffuses into and mixes with water because of their mutual solubility. At the same time hydrophobic PCL blocks are phased out and undergo intrachain contraction and interchain association in water to form core-shell-like micelles stabilized by the swollen hydrophilic PEO blocks. It is helpful to note that there always exists a possibility of forming intermicelle aggregates; namely, the two PCL blocks of a copolymer chain insert into two different micelles to form a bridge. This can be avoided or reduced by dilution. The small amount of THF (1%) introduced in the process was removed under a reduced pressure, which had no effect on the stability and size of the resultant polymeric micelles.

**Laser Light Scattering.** A commercial LLS spectrometer (ALV/SP-150 equipped with an ALV-5000 multi- $\tau$  digital time correlator) and a solid-state laser (ADLAS DPY 425 II, output power is 400 MW at  $\lambda = 532$  nm) as the light source was used. The primary beam is vertically polarized with respect to the scattering plane. The details of the LLS instrumentation and theory can be found elsewhere.<sup>13–15</sup> The following is outlined for the convenience of the discussion. In static LLS, the angular dependence of the absolute time-averaged scattered light intensity, known as the excess Rayleigh ratio ( $R_{vv}(q)$ ), of a sufficiently dilute polymer solution at concentration  $C$  (g/mL) and scattering angle  $\theta$  can be measured.  $R_{vv}(q)$  is related to the weight-averaged molar mass  $M_w$  and the scattering vector  $q$  as

$$\frac{KC}{R_{vv}(q)} \approx \frac{1}{M_w} \left( 1 + \frac{1}{3} \langle R_g^2 \rangle q^2 \right) + 2A_2 C \quad (1)$$

where  $K = 4\pi(dn/dc)^2/(N_A \lambda^4)$  and  $q = (4\pi/\lambda) \sin(\theta/2)$  with  $N_A$  and  $\lambda_0$  being Avogadro's number and the wavelength of light in a vacuum, respectively,  $A_2$  is the second virial coefficient, and  $\langle R_g^2 \rangle_z^{1/2}$  (or written as  $\langle R_g \rangle$ ) is the root-mean-square  $z$ -average radius of gyration of the polymer. By measuring  $R_{vv}(q)$  at different  $C$  and  $q$ , we can determine  $M_w$ ,  $R_g$ , and  $A_2$  from a Zimm plot which incorporates both the extrapolations of  $q \rightarrow 0$  and  $C \rightarrow 0$  on a single grid.

In dynamic LLS, the intensity-intensity-time correlation function [ $G^{(2)}(t) = \langle I(0) I(t) \rangle$ ] in the self-beating mode can be measured, which is further related to the normalized first-order electric field-electric field time correlation function  $g^{(1)}(t) = [\langle E(0) E(t) \rangle / \langle E(0) E^*(0) \rangle]$  as  $G^{(2)}(t) = A[1 + \beta |g^{(1)}(t)|^2]$ . The cumulant analysis of  $G^{(2)}(t)$  can result in an accurate

average characteristic line width ( $\langle \Gamma \rangle$ ). For a pure diffusive relaxation,  $\langle \Gamma \rangle$  is of narrowly distributed micelles related to the average translational diffusion coefficient  $\langle D \rangle$  by  $\langle \Gamma \rangle = \langle D \rangle q^2$  or further to the average hydrodynamic radius  $\langle R_h \rangle$  by the Stokes-Einstein equation.

Both the PCL-*b*-PEO-*b*-PCL micelle dispersion and the lipase PS aqueous solution were clarified by a 0.45  $\mu$ m Millipore filter. In a typical enzymatic biodegradation experiment, a proper amount of dust-free lipase PS aqueous solution was added into 2 mL of dust-free polymeric micelles dispersion to start biodegradation. All biodegradation were conducted inside the LLS cuvette at  $T = 37$  °C.  $R_{vv}(q)$ ,  $G^{(2)}(t)$ , and pH values were simultaneously and in situ measured during the enzymatic biodegradation.

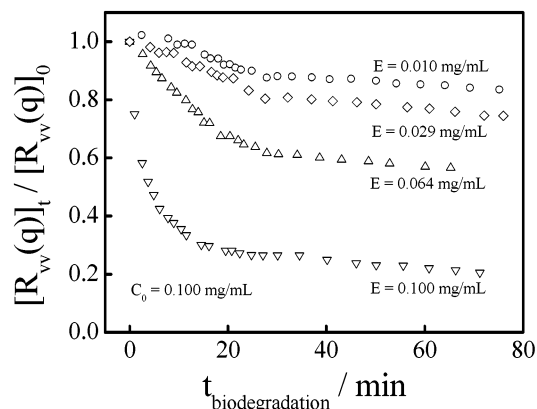
## Results and Discussion

Table 1 summarizes the values of  $M_w$  and  $\langle R_g \rangle$  of different resultant copolymer micelles. The values of  $M_w$  are apparent because they were obtained with a dilute concentration ( $10^{-4}$  g/mL). For such micellar dispersions, the value of the second virial coefficient  $A_2$  is fairly small because water is not a good solvent. The estimated error of  $q \rightarrow 0$  and  $C \rightarrow 0$  is no more than 5%. It is helpful to note that there exist two types of possible particle structures for  $A_m B_n A_m$  triblock copolymers when the solvent is selectively good for the middle block. One is a well-defined flowerlike micelle formed by a close association of all A blocks inside the core-shell-like micelle, while another involves intermicelle association in which the two A blocks of one copolymer chain are inserted into two different micelles.<sup>16,17</sup>

In the close association, it is also likely that some of the A blocks are not in center, but stick out, on the shell. When the B and two A blocks are sufficiently long, the intrachain associations can become dominate in dilute dispersion because the loss of entropy can be compensated by the decrease of enthalpy. This explains the increase of  $\langle R_h \rangle$  with the length of the PCL block. However, when the PCL block is too short to provide a sufficiently strong interaction to match the entropy loss in the intrachain association, the possibility of the intermicelle association increases. This is why there exist two different kinds of aggregations for PCL19. The larger particles are formed due to the intermicelle association, while the smaller ones contain only the intrachain association of the PCL blocks. As expected, the number of the polymeric micelles increases with the copolymer concentration.

On the other hand, it is well-known that the ratio of radius of gyration to hydrodynamic radius ( $\langle R_g \rangle/\langle R_h \rangle$ ) is related to the spatial density distribution and the degree of draining of a scattering object in solution or dispersion; namely,  $\langle R_g \rangle/\langle R_h \rangle \sim 0.774$  for a uniform and nondraining hard sphere,  $\sim 1.0$  for a thin-wall hollow sphere,  $\sim 1.0$ – $1.3$  for a branching chain,  $\sim 1.5$  for a linear random-coil chain in good solvent, and  $\sim 2$  for a worm-like or rodlike chain.<sup>8</sup> For a nondraining core-shell particle,  $\langle R_g \rangle/\langle R_h \rangle$  is less than 0.774 if the core is denser than the shell.<sup>9</sup> As shown in Table 1, the values of  $\langle R_g \rangle/\langle R_h \rangle \sim 1.1$  indicate that the micelles do not have an expected perfect core-shell structure, but a branching structure in which not every PCL block is folded back into the core. The stretching out of these PCL blocks increases  $\langle R_g \rangle$  but has little effect on  $\langle R_h \rangle$  due to the draining, which leads to a higher  $\langle R_g \rangle/\langle R_h \rangle$ .

The decrease of the relative scattering intensities [ $R_{vv}(q)/[R_{vv}(q)]_0$ ] in Figure 1 reveals the biodegradation. On the basis of eq 1, the decrease of  $R_{vv}(q)$  can be



**Figure 1.** Biodegradation time dependence of relative Rayleigh ratio  $[R_{vv}(q)]_t/[R_{vv}(q)]_0$  of PCL19 micelles at 37 °C, where the subscripts "0" and "t" represent time  $t = 0$  and  $t = t$ , respectively, and  $E$  is the enzyme concentration.

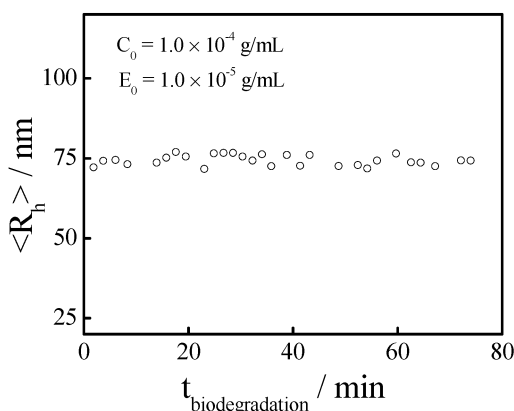


**Figure 2.** Biodegradation time dependence of average hydrodynamic radius  $\langle R_h \rangle$  of PCL19 micelles at 37 °C, where the subscripts "0" and "t" represent time  $t = 0$  and  $t = t$ , respectively.

attributed to the decrease of either the molar mass ( $M$ ) or concentration ( $C$ ) of the polymeric micelles if we ensure that the micelles are monodisperse. It is helpful to note that  $C$  is further proportional to  $M$  and the number of the micelles ( $N$ ), i.e.,  $R_{vv}(q) \propto M^2 N$ . Therefore, in the presence of a mixture of large micelles and small acids generated from the biodegradation, LLS can only detect the remaining nondegraded micelles with a much higher molar mass. In Figure 2, the time-independent average hydrodynamic radius  $\langle R_h \rangle$  of the remaining nondegraded micelles indirectly shows that there is no change in their molar mass ( $M$ ) during the biodegradation. Therefore, the decrease of  $R_{vv}(q)$  in Figure 1 can only be attributed to the decrease of the particle concentration or number; namely,  $[R_{vv}(q)]_t/[R_{vv}(q)]_0 = N/N_0$ .

Figure 3 reveals that the initial rate of the degradation ( $v_{0,LLS}$ ) determined from  $[R_{vv}(q)]_t$  vs  $t$  linearly increases with the enzyme concentration. The line represents a least-squares fitting of  $v_{0,LLS}$  ( $\mu\text{g/mL}\cdot\text{min}$ ) =  $3.98 \times 10^{-2} E_0$  ( $\mu\text{g/mL}$ ). A combination of Figures 1 and 3 shows that not only  $v_0$ , but also the extent of the degradation, increase with the enzyme concentration, suggesting that some lipase PS enzyme molecules gradually lose their activity during the biodegradation, presumably surrounded by the remaining PEO chains which act as surfactant. On the other hand, Figure 4 shows that, for a given lipase PS concentration  $E_0$ , the initial rate  $v_0$  is nearly independent of  $C_0$ , indicating

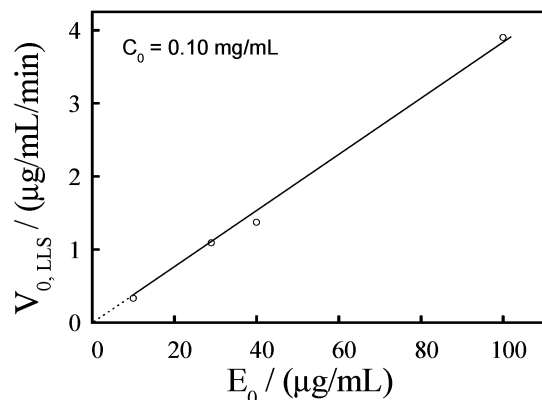


**Figure 3.** Enzyme concentration dependence of initial biodegradation rate ( $v_0$ ) of PCL19 micelles at 37 °C, where  $V_0$  is defined as  $[dC/dt]_{t=0}$ .

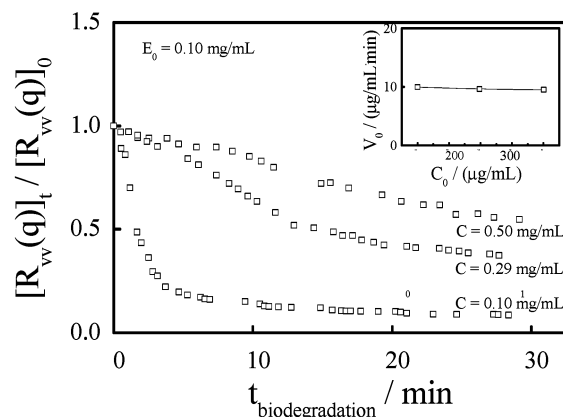


**Figure 4.** Initial copolymer concentration dependence of relative Rayleigh ratio  $[R_{vv}(q)]_t/[R_{vv}(q)]_0$  of PCL19 micelles. The inset shows initial copolymer concentration dependence of initial biodegradation rate ( $v_0$ ).

that the initial degradation follows the zeroth-order kinetics in terms of the polymer concentration. Therefore,  $v_{0,LLS} \propto E_0$ . A combination of Figures 2–4 reveals that the biodegradation is not an all-or-none, but a random one-by-one process, because there is no change in the hydrodynamic radius  $\langle R_h \rangle$  of the remaining micelles. This is just like chemical reaction of small molecules in solution; namely, the degradation occurs when an enzyme molecule meets a micelle, and the degradation of each micelle is too fast to be followed by LLS. Otherwise, we would detect the decrease of  $\langle R_h \rangle$  if all the micelles start to degrade at the same time.

Figure 5 shows that the initial degradation rate ( $v_{0,LLS}$ ) increases with an increasing PCL content. This is expected because lipase PS can only interact with the PCL core, and the hydrophilic PEO shell should have no effect on the biodegradation. It implies a loose structure of the PEO shell so that lipase PS can penetrate the shell to react with the core to induce the degradation. Note that the PEO shell should have a steric hindrance toward the lipase PS. The lack of the PEO effect on the biodegradation indicates that the hindrance is not a rate-determining factor and significant compared to a chemical barrier for the bioreaction of lipase PS itself. Since LLS detects the degradation only when a micelle is completely broken and disintegrated, we have no information about the degradation inside each micelle. Therefore, we further studied the degradation in terms of the change of acidity of the dispersion by a pH meter. This is because the degrada-

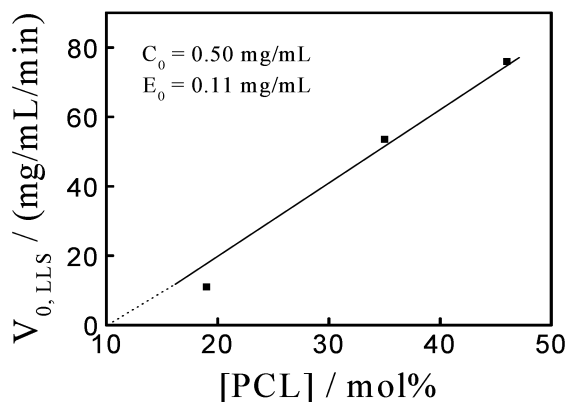


**Figure 5.** Copolymer composition dependence normalized initial biodegradation rate ( $v_0$ ) of PCL19, PCL35, and PCL46 micelles at 37 °C.

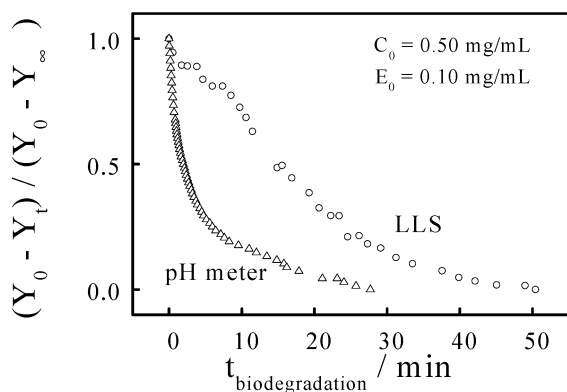


**Figure 6.** Biodegradation time dependence of relative pH and Rayleigh ratio changes of PCL19 micelles, where  $Y$  is  $-\text{pH}$  value or  $R_{\text{v}}(q)$ .

tion of each ester bond on the copolymer chain will produce an acid.

Figure 6 shows that the biodegradation monitored by the change of pH is much faster than that by the change of  $R_{\text{v}}(q)$  under the same experimental condition. The apparent discrepancy is due to different natures of the two methods. The value of pH directly reflects how many ester bonds on the PCL chains have degraded into small acids. It is expected that only when the degradation of the chains inside each micelle reaches a certain extent, the micelle starts to break or disintegrate. This is why the biodegradation observed in LLS is "slower". The apparent discrepancy reveals that the PCL blocks in the copolymer chains are first degraded, and then the dissociation of the chains slowly follows. This is reasonable because the degradation of the PCL blocks reduces the attractive interaction between the chains inside the micelle. Figure 7 shows that the initial rate  $v_{0,\text{pH}}$  determined by a pH meter is also a linear function of the enzyme concentration. The line represents a least-squares fitting of  $v_{0,\text{pH}} \text{ (mol/L/min)} = 9.79 \times 10^{-3} [E_0] \text{ (g/mL)}$ . On the other hand, Figure 8 shows that the initial degradation rate ( $v_{0,\text{pH}}$ ) linearly increases with the PCL content, revealing that  $v_{0,\text{pH}} = [\text{PCL}]E_0$ . Figure 9 shows that for a given lipase PS concentration  $[E_0]$ , the initial rate  $v_0$ , defined as  $d(\text{pH})/dt$ , increases with the initial copolymer concentration  $C_0$ , which is apparently different from the result from laser light scattering in Figure 4. The difference indicates that the degradation of the PCL blocks follows the first-order kinetics in terms of  $C_0$  while the degradation-and-dissociation rate of the polymeric micelles is independent of the

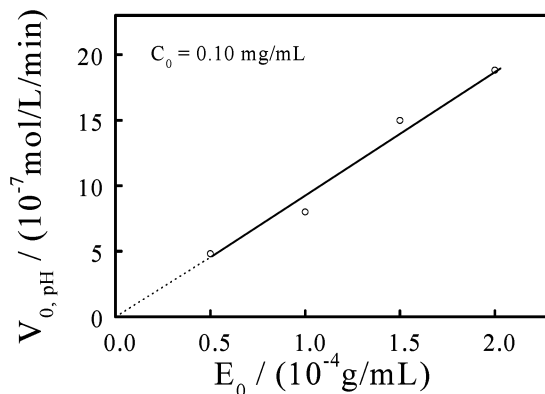


**Figure 7.** Enzyme concentration dependence of initial biodegradation rate ( $v_0$ ) of PCL19 micelles at 37 °C.

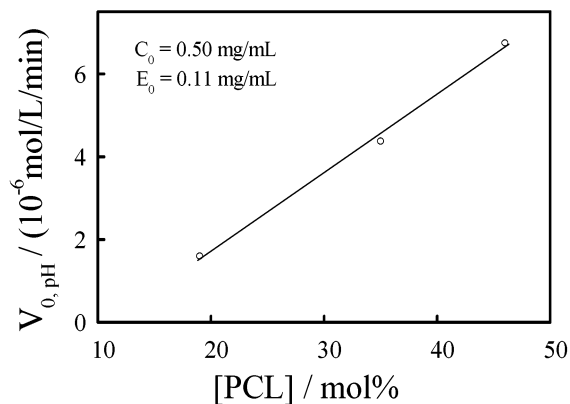


**Figure 8.** Copolymer composition dependence of initial biodegradation rate ( $v_0$ ) of PCL19, PCL35, and PCL46 micelles at 37 °C.

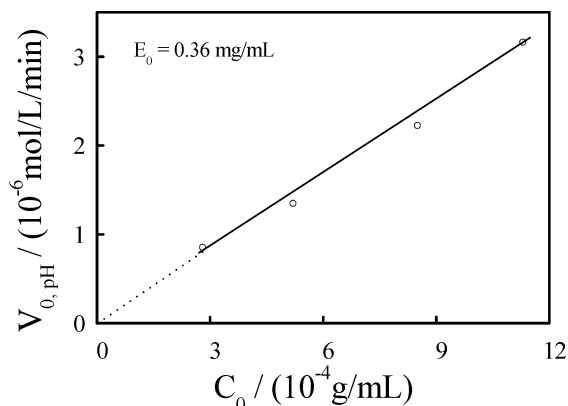


**Figure 9.** Copolymer concentration dependence of initial biodegradation rate ( $v_0$ ) of PCL19, PCL35, and PCL46 micelles at 37 °C.

initial copolymer concentration. This can be attributed to the fact that the initial number of the micelles increases with the copolymer concentration.

## Conclusions

Four PCL-*b*-PEO-*b*-PCL triblock copolymers with different PEO/PCL molar ratios were synthesized. The copolymers can form core-shell-like polymeric micelles in aqueous solution. Using a combination of laser light scattering and pH measurements, we characterized these PCL-*b*-PEO-*b*-PCL micelles and studied their biodegradation in water. The results revealed that the biodegradation of such copolymer micelles can be effectively monitored by a pH meter, while laser light

scattering only detects the overall disintegration of the copolymer micelles after the degradation of the PCL core made of the PCL blocks. Early LLS results on the biodegradation of PCL homopolymer/copolymers should be reconsidered. The change of pH provides a direct and simple detection of the biodegradation of polymer chains as long as it releases  $-\text{COOH}$  during the degradation. Our kinetic study of the degradation of PCL-*b*-PEO-*b*-PCL micelles reveals that the initial degradation rate is proportional to the PCL content and the enzyme and copolymer concentrations.

**Acknowledgment.** This study was supported by the Shanghai-Hong Kong Joint Laboratory in Chemical Synthesis and the Hong Kong Research Grants Council Earmarked Grants (CUHK 4267/00P, 2160136 and CUHK4266/00P, 2160135). Nie thanks the Croucher Foundation (Hong Kong) for a postgraduate studentship. We also thank Prof. Changtao Qian and Prof. Yong Tong for helpful discussions.

### References and Notes

- (1) Schindler, A. *Contemp. Top. Polym. Sci.* **1977**, 2, 251.
- (2) Lewis, D. H.; Chassin, M.; Larger, R., Eds. *Biodegradable Polymers as Drug Delivery Systems*; Marcel Dekker: New York, 1990; p 1.
- (3) Mauduit, J.; Vert, M. *S.T.P. Pharma Sci.* **1993**, 3, 197.
- (4) Wagner, E.; Zenke, M.; Cotton, M.; Beug, H.; Birnstiel, M. L. *Proc. Natl. Acad. Sci. U.S.A.* **1990**, 87, 3410.
- (5) Tuzer, Z.; Kratochvil, P. In *Surface and Colloid Science*; Plenum Press: New York, 1993; Vol. 15, p 1.
- (6) Chu, B. *Langmuir* **1995**, 11, 414.
- (7) Xu, R.; Winnik, M. *Macromolecules* **1991**, 24, 87.
- (8) Liu, T.; Zhou, Z.; Wu, C.; Chu, B.; Schneider, D. K.; Nace, V. M. *J. Phys. Chem. B* **1997**, 101, 8808.
- (9) Zhao, Y.; Liang, H. J.; Wang, S.; Wu, C. *J. Phys. Chem. B* **2001**, 105, 848.
- (10) Zhao, Y.; Hu, T.; Lv, Z.; Wang, S.; Wu, C. *J. Polym. Sci., Polym. Phys. Ed.* **1999**, 37, 3288.
- (11) Gan, Z.; Jim, Y. F.; Li, M.; Zhao, Y.; Wang, S.; Wu, C. *Macromolecules* **1999**, 32, 590.
- (12) Storey, R. E.; Sherman, J. W. *Macromolecules* **2002**, 35, 1504.
- (13) Chu, B. *Laser Light Scattering*, 2nd ed.; Academic Press: New York, 1991.
- (14) Wu, C.; Siddiq, M.; Woo, K. F. *Macromolecules* **1995**, 28, 4914.
- (15) Bo, S.; Yang, H.; Chen, T. *Funct. Polym.* **1991**, 4, 147.
- (16) Zhou, Z.; Chu, B.; Nace, V. M.; Yang, Y.-W.; Booth, C. *Macromolecules* **1996**, 29, 3663.
- (17) Martini, L.; Attwood, D.; Collett, J. H.; Nicholas, C. V.; Tandekaew, S.; Deng, N. J.; Heatley, F.; Booth, C. *J. Chem. Soc., Faraday Trans.* **1994**, 90, 1961.

MA035131+